Tuning of gold nanoparticles plasmon resonances by experiment and simulation

F. TODERAS[a], M. BAIA[a], V. FARCAU[a*], S. ASTILEAN[a], S. ULINICI [b]

[a]Nanobiophotonics Laboratory, Institute for Interdisciplinary Experimental Research, Babes-Bolyai University, Treboniu Laurian 42, 400271, Cluj-Napoca, Romania
[b]ICPE Bistrita SA, Parcului 7, 420035, Bistrita, Romania

We demonstrate, both experimentally and theoretically, the tunability of surface plasmon resonances of gold nanoparticles as function of their size and shape (spheres, rods). Transmission electron microscopy and UV-VIS absorption were employed for experimental characterization. The discrete dipole approximation (DDA), in which the nanoparticle is discretized into a cubic array of polarizable elements, with each element representing the polarizability of a discrete volume of material, is used for simulation of surface plasmon resonances. From simulated and experimental spectra, it is clearly deduced that changes in size and shape of nanoparticle as well as in their local environment can introduce marked changes in their optical properties. The comparison with experiments shows that classical electromagnetic theory works well, provided that we have size distribution values of particle dimensions and provided that the dielectric environment is properly characterized and modeled.

1. Introduction

At the nanoscale, materials exhibit unique optical, electronic, and magnetic properties that are not observed at the bulk scale. For example, noble metal nanoparticles exhibit strong optical extinction at visible wavelengths due to localized surface plasmon resonances SPR (i.e., collective oscillation of the conduction band electrons upon light absorption). Indeed, gold nanospheres of diameter smaller than 100 nm appear red (not gold!) when suspended in transparent media. In the case of particles having various shapes, several plasmon resonance modes appear associated with the various orientations of the particle axes. These different oscillation modes can be also observed when the particles are randomly dispersed in solution. In general, the optical properties of noble metal nanoparticles are tunable throughout the visible and near-infrared region of the spectrum as a function of their size, shape, aggregation state, and local environment [1].

Gold nanoparticles can be easily synthesized by chemical methods and offer, in addition to their enhanced absorption and scattering, good biocompatibility and conjugation to a variety of biomolecular ligands or antibodies making them suitable for use in biochemical sensing and detection, medical diagnostics and therapeutic applications [2-5].

In order to understand the optical response of noble-metal nanoparticles, a number of theoretical approaches, including the Mie theory [6] for spherical and ellipsoidal forms, discrete dipole approximation (DDA) [7, 8] or finite difference time domain methods (FDTD) [9] for arbitrary shape particles, have been used. The discrete dipole approximation, DDA, is a computational procedure suitable for studying scattering and absorption of electromagnetic radiation by particles with sizes on the order of, or less than, the incident light wavelength, and especially for nonspherical shapes [8].

In this paper, the synthesis of gold nanoparticles of different size and shape is made in water solution at various conditions. The optical properties are tuned from the Mie resonance for spherical nanoparticles (519 nm) to double resonances located on nanorods (519 and 680 nm). The comparison between the optical studies obtained experimentally and by DDA simulation gives a direct proof of the change in the optical properties of as prepared gold nanoparticles with their size and shape, and it reinforces the accuracy of the DDA simulation.

2. Experimental

In our experimental protocol, the following reagents were used: tetrachloroauric acid ($HAuCl_4$), trisodium citrate, cetyltrimethyl ammonium bromide (CTAB), sodium borohydride, silver nitrate and ascorbic acid from Merck, Germany.

For the synthesis of spherical gold nanoparticles, the citrate reduction method has been employed as described in literature [10, 11]. Two colloidal suspensions with particle of diameter of 18±2 nm and 40±2 nm, respectively, were prepared by controlling the relative proportions of reagents.

For the synthesis of gold nanorods, a seed-mediated growth method, which is a two-steps procedure, has been employed [12]. In the first step a seed spheres solution of 3-5 nm gold nanocrystals was prepared. In the second step,

the growth of gold nanorods from as prepared seed nanoparticles in presence of CTAB, sodium borohydride, $AgNO_3$ and ascorbic acid was used. The nanorods were concentrated and separated from solution by centrifugation. The supernatant, containing mostly CTAB molecules and gold ions, was removed and the solid part containing rods was redispersed in ultrapure water. The as synthesized nanorods in water are coated with a bilayer of CTAB molecule being stable at room temperature for many months. Two colloidal suspensions of nanorods of aspect ratio of 2.4 and 3, respectively, were prepared. The nanorods are characterized by the aspect ratio defined as the ration between their longitudinal and transversal size.

A JEOL JEM 1010 transmission electron microscope was used to determine the gold nanoparticles size and shape. The UV–VIS absorption spectra of colloidal solution were recorded with a Jasco V-530 UV–VIS spectrophotometer using unpolarized light with a probe beam size of approximately 3–4 mm^2.

3. Simulation

The optical response (absorption, scattering, near field value) of noble metal nanoparticles can be obtained in principle by solving Maxwell's equations. The exact solution for a homogeneous spherical particle was found by G. Mie in 1908 [13]. However, the exact solutions for particles with arbitrary shapes are not straightforward, and approximations are needed to be considered. The DDA is an approximation tool which provides a convenient method for describing light scattering from nanoparticles of arbitrary shapes. This method was first proposed by Purcell and Pennypacker [14], who used it to study interstellar dust grains. In the DDA, the object of interest is represented as a cubic array of N polarizable elements. The response of this array to an applied electromagnetic field is described by self-consistently determining the induced dipole moment in each element. This information can be used to determine far-field properties like extinction efficiencies and also near-field properties especially the electromagnetic field (E-field) near the particle surface [8]. In this approximation, each dipole represents the polarizability of a particular sub-volume of target material. Purcell and Pennypacker used the Clausius-Mossotti polarizability:

$$\alpha^{CM} = \frac{3d^3}{4\pi}\frac{\varepsilon_j - 1}{\varepsilon_j + 2}, \qquad (1)$$

where ε_j is the dielectric function of the target material at location r_j and d represent the lattice of a DDA cell of volume $V=d^3$. Draine and Goodman [15] introduced the following corrected polarizabilities:

$$\alpha^{LDR} \approx \frac{\alpha^{CM}}{1+(\alpha^{CM}/d^3)[(b_1 + m^2 b_2 + m^2 b_3 S)(kd)^2 - (2/3)i(kd)^3]}, \quad (2)$$

$$b_1 = -1.891531, \qquad b_2 = 0.1648469,$$
$$b_3 = -1.7700004, \qquad S = \sum_{j=1}^{3}(\hat{a}_j\hat{e}_j)^2$$

where $\hat{a}_j$ and $\hat{e}_j$ are unit vectors defining the incident direction and the polarization state, d represent the interdipole spacing and $k=\frac{2\pi}{\lambda}$ represent the wave vector. Each dipole has a polarization $P_j = \alpha_j E_j$, where E_j is the electric field at r_j that is due to the incident wave $E_{inc,j} = E_0 \exp(ik \cdot r_j - i\omega t)$ plus the contribution of each of the other N-1 dipoles:

$$E_j = E_{inc,j} - \sum_{k \neq j} A_{jk}P_k , \qquad (3)$$

where $-A_{jk}P_k$ is the electric field at r_j.

The extinction and absorption cross sections C_{ext} and C_{abs} were evaluated [16]:

$$C_{ext} = \frac{4\pi k}{|E_o|^2}\sum_{j=1}^{N} \text{Im}(E_{inc,j}^* \cdot P_j), \qquad (4)$$

$$C_{abs} = \frac{4\pi k}{|E_o|^2}\sum_{j=1}^{N}\left\{\text{Im}[P_j \cdot (\alpha_j^{-1})^* P_j^*] - \frac{2}{3}k^3|P_j|^2\right\} \qquad (5)$$

This method is known to be one of the most powerful and flexible electrodynamics methods for calculating the optical response of particles with arbitrary shapes. For our calculations we have used the DDA code developed by Draine and Flatau [17], called DDSCAT. In the case of the sphere we considered unpolarized light, and for the nanorod we took two polarizations of incident light, one parallel to the long axis of the particle, and the other perpendicular to it. The size of particle of arbitrary shape and volume V is specified by its effective radius:

$$r_{eff} = (3V/4\pi)^{1/3} \qquad (6)$$

which represents the radius of a sphere having an equal volume to that of the particle. If the target is represented by an array of N dipoles, located on a cubic lattice with lattice spacing d, then $V = Nd^3$. In the case of the nanorod, we additionally define the size aspect ratio (R), which is the ratio of the nanorod's long axis to the short one. In all calculations the refractive index of the surrounding medium was consider to be n=1.33 + 0i (water) for all wavelengths. For the dielectric constants of gold we used the ones measured by Johnson and Christy [18]. A number of 11536 dipoles were used to approximate the sphere, and 12000 dipoles for gold nanorod considered of cylindrical geometry. The quantity which is calculated by the program is $Q_{abs} = C_{abs}/\pi r_{eff}$.

We checked the accuracy of our DDA results for spherical particles and found that the DDSCAT program provides a

good convergence to the Mie theory in the limit when the particle size is much smaller compared with the wavelength: $|n|kD \leq 1$, where n is the surrounding refractive index and D is the diameter of particles.

5. Results and discussion

Figure 1 (A) shows TEM image of gold nanospheres and reveals that the nanoparticles are quite uniform in their size, with an average diameter of 18 ± 2 nm. A TEM image of the nanorods is shown in fig. 1 (B) where the rods are of 50 ± 6 nm in length and of 24 ± 4 nm in diameter. Small numbers of spherical or cubical shape particles are still found in nanorods batch.

The optical spectrum of gold nanospheres in water suspension exhibits a single absorption band attributed to SPR (collective electronic oscillation). Figure 2 (a, b) shows the experimental absorption spectra of colloidal suspensions containing spherical gold nanoparticles of average diameter of 18 and 40 nm respectively. The two maxima of plasmon resonance bands occur at 519 and 533 nm, respectively. The absorption peaks shift to red with the increase of diameter and the bandwidth also changes when the sizes changes.
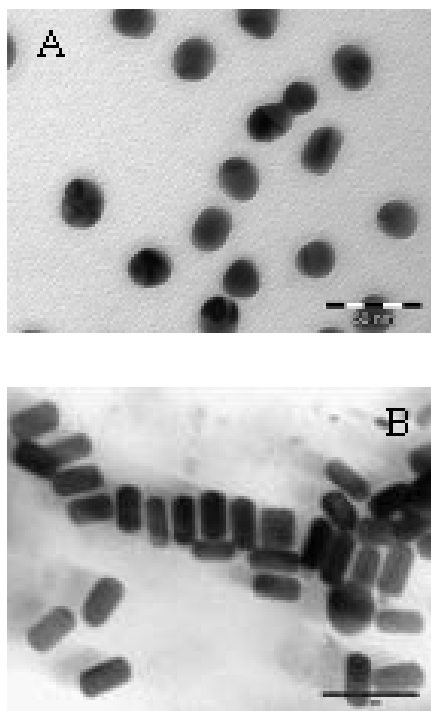

Fig. 1. TEM pictures of (A) gold nanospheres of 18 nm in diameter and (B) gold nanorods of 2.4 aspect ratio.

These optical properties accounting for the surface plasmon resonance can be theoretically explained by the Mie theory. Indeed, for a spherical object, electrodynamic calculations give a series of multipole oscillations (dipole,

quadrupole, etc.) for the absorption and scattering cross section as a function of the particle radius. The extinction spectrum is composed of the sum of absorption and scattering modes, each of which has a relative contribution that depends on the particle size. Higher-order modes become more dominant with increasing particle size causing the plasmon absorption band to redshift while the bandwidth increases [19].
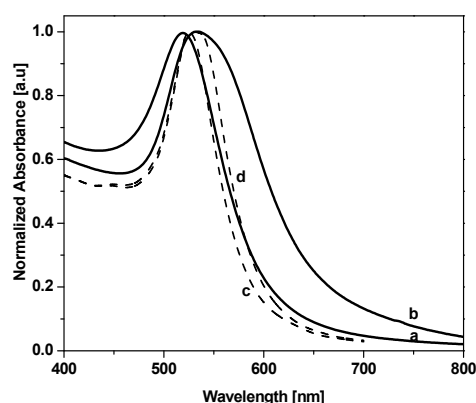

Fig. 2. The UV-VIS absorption spectra of colloidal gold nanospheres of (a) 18 nm and (b) 40 nm diameter (solid line). The calculated spectra of gold nanospheres of (c) 18 nm and (d) 40 nm diameter (dashed line).

Additionally to the analytical computation given by an analytical Mie formula, we performed DDA calculations. In Figure 2, the dotted spectra represent the calculated absorption efficiency: gold nanospheres of 18 nm diameter exhibits a maximum at 521 nm (spectrum (c)) while gold nanospheres of 40 nm diameter, exhibits its maximum at 528 nm (spectrum (d)). Normalization of spectra has been made for a better comparison between the absorption maximum of theoretical and experimental spectra. The small differences observed between two maxima of experimental and calculated spectra are reasonable and can be explained as follows. In the case of simulation, the spectra are narrow and slightly shifted due to the fact that we consider for calculation only identical (mono-disperse) spherical nanoparticles in aqueous media. However, the experimental method does not provide solution of perfectly spherical, mono-disperse and totally non-interacting particles (Fig. 1 A). Further, the synthesized nanoparticles are coated with a citrate layer and the refractive index of the surrounding medium should be slightly different from the theoretical refractive index, as aqueous medium contains different ions which derive from the reaction medium and therefore. Thus, the difference in position and bandwidth of absorption spectra can be entirely explained by contributions from the variation of local refractive index and the degree of dispersity and aggregation of particles in solution.

When the shape of the nanoparticle changes from spherical to elongated shape like rod, the surface plasmon resonances change dramatically. As result, the UV–vis spectrum of gold nanorod exhibit two plasmon resonance

bands instead of single resonance as in the case of spherical particles. The band situated at high frequency (or low wavelength) is referred to as the transversal plasmon resonance while the band situated at low frequency (or high wavelength) is called the longitudinal plasmon absorption. Examples of such experimental and theoretical spectra are presented in Fig. 3.
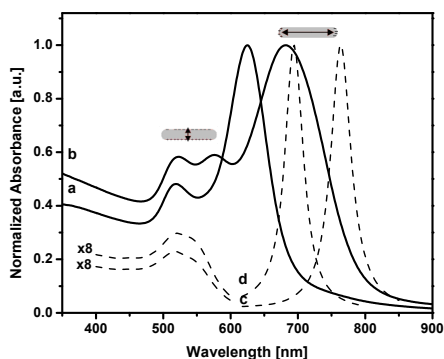

Fig. 3. The UV-VIS absorption spectra of colloidal gold nanorods with average aspect ratio of (a) 2,4 and (b) 3 (solid line) . The calculated spectra of gold nanorods with aspect ratio (c) 2.4 and (d) 3 (dashed line)

The absorption of the gold nanorod is very sensitive to the aspect ratio of rods. As soon as the aspect ratio of nanorods changes from 2.4 to 3, the longitudinal absorption maximum is shifted from 625 nm to 680 nm. This should occur also for the transversal plasmon resonance. However, in our case the transverse plasmon absorption band situated at 519 nm is apparently insensitive to the aspect ratio. This behavior is due to the fact that the transversal dimension of rods in both cases coincide each other and also with the size gold nanospheres (see Fig. 1).

Theoretical calculations were performed by DDSCAT computer code for nanorods of aspect ratio 2.4 and 3, respectively, dispersed in water. The two expected maxima were found in the simulated spectra, corresponding to the transverse and longitudinal surface plasmon resonance, respectively (Fig. 3 (c,d)). The position of calculated perpendicular mode coincides very well with the experimental spectra of colloids in the case of both aspect ratios. However, in the experimental spectra, the band intensity is much stronger that the calculated and the result could be understood by some extra contribution from spherical particles which should be present in solution. Apart that it is obvious that the length of nanorod has taken control over the location of the second peak, namely the longitudinal peak. The calculated plasmon resonance corresponding to the mode with the electric field parallel to the nanorod axis is shifted to red relatively to the experimental peak and the shift is much important than in the case of spherical particles (see Fig. 2 and Fig. 3). It is clear that the band position should depend on the refractive index of environmental medium. However, in our opinion this effect is not enough to explain such large shift between experimental and theoretical peaks. As the growth mechanism of nanorods is not well established it is difficult to estimate to what extent the presence of the coating surfactant and crystallinity can modify the optical properties of nanorods.

6. Conclusions

The experimental and theoretical results presented here indicate that it is now possible to describe many optical properties of noble metal nanoparticles having anisotropic shapes in complex dielectric environments. The comparison with experiments shows that classical electromagnetic theory works well, provided that we have size distribution values of particle dimensions and provided that the dielectric environment is properly characterized and modeled. This work has emphasized comparisons only with experiment for extinction spectra.

We emphasize that we calculated the optical properties of particles that are sufficiently dispersed that they may be treated as being isolated. However, particle interactions are important, and sometimes they are dominant. The calculation of such properties, as for example surface enhancement Raman scattering (SERS) intensities, provides new challenges that are an important component of our current research.

References

[1] M. Hu, J. Chen, Zhi-Yuan Li, L. Au, G. V. Hartland, X. Li, M. Marquez and Y. Xia, Chem. Soc. Rev. **35**, 1084, (2006).
[2] N. L. Rosi, C. A. Mirkin, Chem. Rev. **105**, 1547 (2005).
[3] J. C. Riboh, A. J. Haes, A. D. McFarland, C. Ranjit, R. P. Van Duyne, J. Phys. Chem. B **107**, 1772, (2003).
[4] M. Baia, F. Toderas, L. Baia, J. Popp, S. Astilean, Chem. Phys. Lett. **422**, 127 (2006).
[5] F. Toderas, M. Baia, L. Baia, S. Astilean, Nanotechnology, **18**, 255702 (2007).
[6] C. Sonnichsen, T. Franzl, T. Wilk, G. von Plessen, J. Feldmann, New Journal of Physics **4**, 93.1 (2002).
[7] C. Noguez, J. Phys. Chem. C **111**, 3806 (2007).
[8] P. K. Jain, K. S. Lee, I. H. El-Sayed, M. A. El-Sayed, J. Phys. Chem. B **110**, 7238 (2006).
[9] N. N. Nedyalkov, P. A. Atanasov, M. Obara, Nanotechnology **18**, 305703, (2007).
[10] C. D. Keating, M. D. Musick, M. H. Keefe, M. J. Natan, J. Chem. Educ., **76**, 949 (1999).
[11] G. Frens, Nat. Phys. Sci. **241**, 20 (1973).

[12] N. R. Jana, L. Gearheart, C. J. Murphy, J. Phys. Chem. B **105**, 4065, (2001).

[13] G. Mie, Ann. Phys. (Leipzig)**, 25,** 377 (1908)

[14] E. M. Purcell; C. R. Pennypacker, Astrophys. J. **186**, 705 (1973).

[15] B. T. Draine; J. Goodman, Astrophys. J., **405**, 685 (1993).

[16] B.T. Draine, Astrophys. J., **333**, 848 (1988).

[17] B. T. Draine, P. J. Flatau, Source Code DDSCAT 6.1, http://www.astro.princeton.edu/~draine/ DDSCAT.html

[18] P. B. Johnson, R. W. Christy, Phys. Rev. B **6,** 4370 (1972).

[19] S. Link, M. A. El-Sayed, Annu. Rev. Phys. Chem., **54**, 331 (2003).

*Corresponding author: cfarcau@phys.ubbcluj.ro